This article has been accepted for publication in a future issue of this journal, but has not been fully edited. Content may change prior to final publication. Citation information: DOI 10.1109/TSP.2016.2582466, IEEE Transactions on Signal Processing

Parameter Estimation of Wideband Underwater Acoustic Multipath Channels based on Fractional Fourier Transform

Yanbo Zhao, Hua Yu, *Member, IEEE,* Gang Wei, *Senior Member, IEEE,* Fei Ji, and Fangjiong Chen

***Abstract*—In the presence of relative motion, the wideband underwater acoustic multipath channel can be more accurately described by a multi-scale multi-lag (MSML) model. The signal components received from different paths can be differentiated in terms of Doppler scales, time delays, and amplitudes. Estimation of these parameters is essential for many underwater applications. In this paper, by virtue of the fractional Fourier transform (FrFT), an accurate and efficient method for parameter estimation is proposed for MSML underwater acoustic channels. The algorithm proceeds in an iterative manner, returning parameter estimates of the most dominant signal component successively. With the linear frequency modulation signal employed as the probe signal, the estimation of the Doppler scale factor of each dominant component can be converted into a process of searching for the optimal fractional angle/order of the received signal's FrFT. At each iteration, a sub-iteration is contained to adjust the optimal fractional order. The pulse compression techniques for LFM signal, in both time domain and FrFT domain, are utilized to obtain precise parameter estimates. Once the parameters of a multipath are estimated, the corresponding component will be separated from the received signal—through eliminating the resampled, delayed and attenuated version of the original probe signal. The sparsity of the underwater acoustic channel is considered to reduce the amount of calculation. Simulation results confirm the effectiveness of the proposed estimation method. It is shown that the proposed algorithm outperforms the existing FrFT domain filter and short-time FrFT domain filter in multicomponent separation. It is also indicated that the proposed parameter estimation is superior to the matching pursuit based method in accuracy.**

***Index Terms*—wideband underwater acoustic channels, channel estimation, fractional Fourier transform, pulse compression.**

Manuscript received April 8, 2015; revised November 24, 2015 and May 25, 2016; accepted May 28, 2016. Date of publication June 10, 2016; date of current version June 10, 2016. The associate editor coordinating the review of this manuscript and approving it for publication was Prof. Joseph Tabrikian. This work was supported in part by the National Natural Science Foundation of China under Grants 61431005, 61327005, 61322108, 61372081 and 61302120, by the Guangdong provincial research project under Grants 2014A030311034, 2015B010101007 and 2016B09091849, and by the Program for New Century Excellent Talents in University under Grant NCET-12-0196. (Corresponding author: Hua Yu)

The authors are with the National Engineering Technology Research Center for Mobile Ultrasonic Detection, South China University of Technology, Guangzhou, 510640 China (e-mail: zhaoyanbobby@foxmail.com; {yuhua, ecgwei, eefjchen, eefeiji}@scut.edu.cn).

Color versions of one or more of the figures in this paper are available online at http://ieeexplore.ieee.org.

Digital Object Identifier 10.1109/TSP.2016.XXXXX

I. Introduction

Acoustic wave has been considered as the most effective medium for signal transmission in underwater detection and communication applications. Meanwhile, the underwater acoustic (UWA) channels are the most complicated wireless channels since they are both frequency-selective and time selective [1]–[4]. In particular, Doppler effect caused by relative motion and varying scatterer velocities is quite serious since the multipath signals along different sound rays are stretched or compressed in time by different Doppler scales [2]–[9]. In a typical terrestrial wireless system, such Doppler effect can be approximated as Doppler shift. For most UWA systems, however, the fractional bandwidth and the time-bandwidth product of the signal are usually so large that the narrowband condition does not hold [2], [4]. Hence, the wideband system model and corresponding parameters should be adopted for UWA applications.

Scale factor, time delay, and complex amplitude of each multipath are the parameters which need to be determined in the wideband UWA channel estimation. Since the scaling changes involve resampling process at the receiver, most existing channel estimation methods only consider and compensate one dominant scale factor [5], [6], [10]. Although it simplifies the receiver structure, such scale compensation mechanism leaves residual sampling errors to other scaled components, and ignores the potential diversity which could be exploited in a time-scale channel characterization to increase communication performance [7], [8]. Therefore, the challenge of parameter estimation of UWA channels lies in identifying individual multipath components with different scale factors from the received signal, which is sampled with an identical sampling rate. So far, there is no extensive research for multiscale factor case.

In [9], the matching pursuit decomposition (MPD) algorithm is utilized to decompose multicomponents with different scale factors. The recursive algorithm returns parameter estimates of each multipath by selecting the atom which has the highest degree of correlation with the residual signal. The residual signal energy decreases significantly after the dominant multicomponents are decomposed and eliminated from the received signal. However, lots of atoms need to be generated and stored to form a signal dictionary beforehand. To guarantee a fine scale resolution, the atom amount could be extremely huge and lead to extensive calculation, especially when the scale spread range is large.

This article has been accepted for publication in a future issue of this journal, but has not been fully edited. Content may change prior to final publication. Citation information: DOI 10.1109/TSP.2016.2582466, IEEE Transactions on Signal Processing

Recently, a method based on fractional Fourier transform (FrFT) is applied extensively to separate the overlapping linear frequency modulation (LFM) signals in all kinds of signal processing applications [11]–[18]. FrFT is a generalization of the classical Fourier transform, and can be interpreted as a rotation in the time-frequency plane [19], [20]. In the FrFT domain, an LFM signal can be represented as an impulse at an appropriate time-frequency rotation angle since the transform kernel is a set of chirp bases. This property makes FrFT suitable for processing LFM (chirp) signals.

In [11], an FrFT-based separation method of overlapping LFM signals is given, but the Doppler scaling change is not considered. In [12], the FrFT is used to compensate a known single Doppler scale of the LFM echoes. In [13], an FrFT-based joint delay and scale estimation—for a single moving target—is developed. The parameters can be estimated by searching for the maximum magnitude of FrFT of the target echo. The multi-scale case is studied in [14] and the parameters (frequency modulation slope, center frequency and amplitude) of each multicomponent are estimated. The delays of the components, however, are not involved. FrFT domain filtering is used to separate the interested components and suppress noise. The multi-scale and multi-lag case is dealt with in [15]. The delay and scale can be determined by estimating the locations and widths of the peaks detected in the FrFT magnitude of the received signal. However, for a single target, the estimation error is larger than the method proposed in [13] at high SNR. What is more, the error could be accumulated when the number of targets increases.

For LFM signal, the key to estimate the scale factor is to find out the optimal fractional order of the received signal's FrFT, or the rotation angle at which the transformed signal reaches a maximum amplitude and forms an impulse. A coarse-to-fine method is proposed to estimate the compact fractional domain in [16]. The optimal fractional order can be obtained by searching the maximum value of the fractional Fourier amplitude spectrum. However, the authors only consider multi-lag (without multi-scale) case or multi-scale (without multi-lag) case, and do not provide any separation techniques.

A problem, usually associates with the discrete signal processing, is ignored in the above literatures. That is the relationship between sampling duration of the observed signal and time duration of the multipath signal. This issue is investigated in [17], but only limited to a single component case. The short-time FrFT (ST-FrFT) is systematically studied in [18]. It could be a possible way to solve the above problem. In addition, an ST-FrFT domain filter is proposed in [18], which has better performance than FrFT domain filter in the multicomponent LFM signal separation. However, the matched-order (optimal fractional order) of each component needs to be known beforehand. Besides, for each component, the length of the short-time window should be carefully predetermined so as to obtain the minimum support in the ST-FrFT domain.

The present paper further explores the parameter estimation of wideband UWA multipath channels, by using the LFM training signals and FrFT. An accurate estimation method is proposed. Its main characteristics are listed as follows,

- The multi-scale multi-lag (MSML) channels are the research objectives.
- The pulse compression techniques of LFM signals, in both time domain and FrFT domain, are employed to obtain precise estimates.
- The relationship—between discrete FrFT section of the sampled received signal and time duration of the individual multipath signal—is considered.
- The relationship—between sampling rate and estimation accuracy—is considered for discrete data processing.

The second item provides a better method for separating the overlapping signal than the existing FrFT domain filter [14] and ST-FrFT domain filter [18]. This will be verified in the simulation. Moreover, the third and fourth items are seldom considered in the above mentioned literatures, but we think they are important and inevitable issues in practice.

The remainder of this paper is organized as follows. The system model is constructed in Section II. In Section III, pulse compression of LFM signals in both time domain and FrFT domain is stated as the parameter estimation principle for single-path channel. In Section IV, an efficient and accurate parameter estimation method for the MSML UWA channels is proposed. Computer simulation is given in Section V, and finally conclusions are drawn in Section VI.

II. System Model

In the literature, the time-varying impulse response of the wideband UWA multipath channel can be modeled as an MSML channel and be expressed as [6], [21]

$$h\left(t,\tau\right)=\sum_{l=1}^{L}A_l(t)\delta\big(\tau-\left(\alpha_l\tau_l-\left(\alpha_l-1\right)t\right)\big) \tag{1}$$

where L is the number of total channel taps, $A_l(t)$, α_l and τ_l are the time-varying amplitude, Doppler scale factor, and time delay of the l-th multipath, respectively. Doppler shifts caused by different scale factors aside, the time dependence of $A_l(t)$ also causes Doppler spread [2]. In this paper, we focus on the effect of scale factors. Thus we assume that the amplitude maintains constant during the transmission of the training signal, i.e. the time dependence parameter $A_l(t)$ reduces to a time independence parameter A_l in (1). Denoting the transmitted signal as $s(t)$, the received signal $r(t)$ without considering noise is given as

$$r(t)=\int_{-\infty}^{\infty}h(t,\tau)s(t-\tau)d\tau=\sum_{l=1}^{L}A_l s\big(\alpha_l\left(t-\tau_l\right)\big) \tag{2}$$

It can be seen that the received signal $r(t)$ is a superposition of multiple scaled and delayed versions of the transmitted signal $s(t)$. Since scale factors and time delays could be differentiated for individual multipaths, such channel is called the MSML channel.

Equation (2) represents the relationship between the received signal and the transmitted signal from the multipath perspective. Also, I/O relationship can be represented from the perspective of delay-scale domain, directly, by discretizing the continuous delay and scale parameters, e.g. [7]. This representation and discretization can be seen in Appendix A.

This article has been accepted for publication in a future issue of this journal, but has not been fully edited. Content may change prior to final publication. Citation information: DOI 10.1109/TSP.2016.2582466, IEEE Transactions on Signal Processing

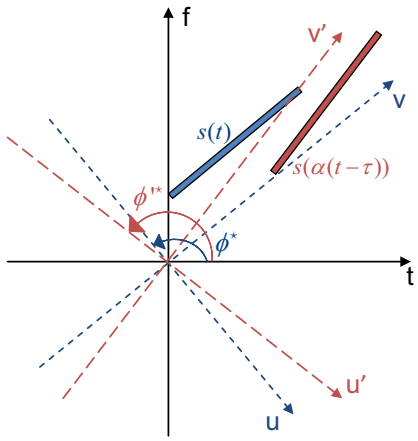

Fig. 1. FrFT of $s(t)$ and $s(\alpha(t-\tau))$. For an LFM signal, there exists an ORA $\phi^\star$, which gathers the LFM signal energy at a certain value on the rotated u-axis, see the dense dotted frame of axes in blue color. Once a time delay and a Doppler scale happen to the LFM signal, the ORA switches to $\phi'^\star$, and the signal forms a new impulse function in the u'-v' FrFT domain, see the loose dotted frame of axes in red color.

UWA multipath channels usually show sparsity both in time domain and frequency domain [6] [9]. It is assumed that only a few taps are significantly nonzero, i.e., L is a small positive integer in (1). This sparse property is useful for reducing the amount of calculation. Therefore, L sets of $\{\alpha_l, \tau_l, A_l\}$ are going to be determined in this paper.

We consider an LFM signal as the channel training signal $s(t)$, which is

$$s(t) = \mathrm{rect}(t) \exp\left(j\left(2\pi f_0 t + \pi k t^2 + \varphi_0\right)\right) \tag{3}$$

where f_0, k and φ_0 are the starting frequency, modulation slope and initial phase, respectively. The stopping frequency is $f_1 = f_0 + kT$, where T is the duration of the signal. The function $\mathrm{rect}(t)$ denotes the normalized rectangular window, i.e. $\mathrm{rect}(t) = 1/T$ for $t \in [0, T]$ and zero otherwise.

III. FrFT-based Parameters Estimation for Single Path Channel

According to (2), when a complex channel attenuation A, a temporal scaling α and a delay τ happen to the LFM signal, the received signal is

$$\begin{aligned} r(t) &= A \cdot s(\alpha(t-\tau)), \\ &= A \cdot \mathrm{rect}(\alpha(t-\tau)) \exp\left(j\left(2\pi f_0' t + \pi k' t^2 + \varphi_0'\right)\right), \end{aligned} \tag{4}$$

with

$$k' = k\alpha^2 \tag{5}$$

$$f_0' = \alpha f_0 - k\alpha^2\tau \tag{6}$$

$$\varphi_0' = \pi k\alpha^2\tau^2 - 2\pi f_0 \alpha\tau + \varphi_0 \tag{7}$$

We can see that the received signal $r(t)$ is still an LFM signal, but with different parameters.

Next, we first estimate the scale factor in term of the change of the modulation slope. Then, we estimate the delay and amplitude through a cross-correlation process.

Algorithm 1 Scanning Algorithm (to get the optimal fractional order corresponding to the maximum FrFT value)

Input:

$\mathbf{r}$ —vector of the samples of the signal to be transformed; γ_r—number of the iteration times, which represents the scanning precision.

Scanning:

1: Initialization: the scanning range set of the fractional order $\mathfrak{O}_r = [0.5, 1.5]$; scanning spacing $s_p = 0.1$;
2: **while** $\gamma_r >= 1$ **do**
3: Compute $p'^\star = \max_{p \in \mathfrak{O}_r}\{\max|F^p\mathbf{r}|\}$;
4: Update $\mathfrak{O}_r = [\max(0.5, p'^\star - s_p/2), \min(p'^\star + s_p/2, 1.5)]$; $s_p = s_p/10$; $\gamma_r = \gamma_r - 1$;
5: **end while**

Output:

The optimal fractional order $p'^\star$ (the ORA $\phi'^\star = p'^\star\pi/2$).

A. Estimation of the Scale Factor

To estimate the scale factor α, we utilize the pulse compression of LFM signals in FrFT domain. The FrFT of a function $x(t)$, with a fractional order p and a rotation angle $\phi = p\pi/2$, is defined as [19] [20]

$$F^p x = X_\phi(u) = \int_{-\infty}^{\infty} x(t) K_\phi(t,u)\, dt \tag{8}$$

where $K_\phi(t,u)$, the transformation kernel, is defined as

$$K_\phi(t,u) = \begin{cases} A_\phi e^{j\pi\left((t^2+u^2)\cot\phi - 2ut\csc\phi\right)}, \text{for } \phi \neq n\pi \\ \delta(t-u), \text{ for } \phi = 2n\pi \\ \delta(t+u), \text{ for } \phi = (2n \pm 1)\pi \end{cases}$$

where the complex amplitude factor $A_\phi = \sqrt{(1 - j\cot\phi)}$, and n is an arbitrary integer.

Denoting the FrFT of $s(t)$ as $F^p s = S_\phi(u)$, an optimal rotation angle (ORA) $\phi^\star$ exists to max the peak amplitude of $F^p s$. Accordingly, $p^\star = 2\phi^\star/\pi$ is called as the optimal fractional order. The $S_{\phi^\star}(u)$ forms a pulse in the FrFT domain, and its peak value appears at $u^\star$. By such time-frequency plane rotation, pulse compression is operated in the FrFT domain. From [22], the relationship between the ORA and the LFM signal frequency modulation slope can be derived as

$$\phi^\star = -\mathrm{arc}\tan\left(\frac{1}{k}\right), \tag{9}$$

i.e.,

$$k = -\cot\phi^\star. \tag{10}$$

Accordingly, the FrFT of the received LFM signal $r(t)$ in (4) also forms a pulse at a new ORA $\phi'^\star$, as shown in Fig.1. Therefore, once the degree of the new ORA $\phi'^\star$ is known, the scale factor estimate, $\hat{\alpha}$, can be obtained since the slope k is known beforehand at the receiver. That is, by combining (5) and (10), the scale factor is estimated by

$$\hat{\alpha} = \sqrt{-\frac{\cot\phi'^\star}{k}}. \tag{11}$$

Searching for the ORA $\phi'^\star$ of $r(t)$ needs numerous FrFT computations and comparisons. Since the received LFM signal

This article has been accepted for publication in a future issue of this journal, but has not been fully edited. Content may change prior to final publication. Citation information: DOI 10.1109/TSP.2016.2582466, IEEE Transactions on Signal Processing

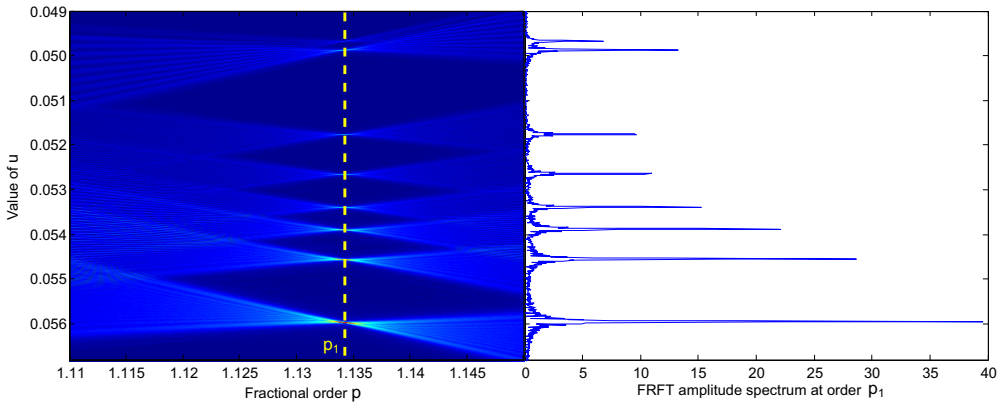

(a) All multipaths undergo one identical scaling change

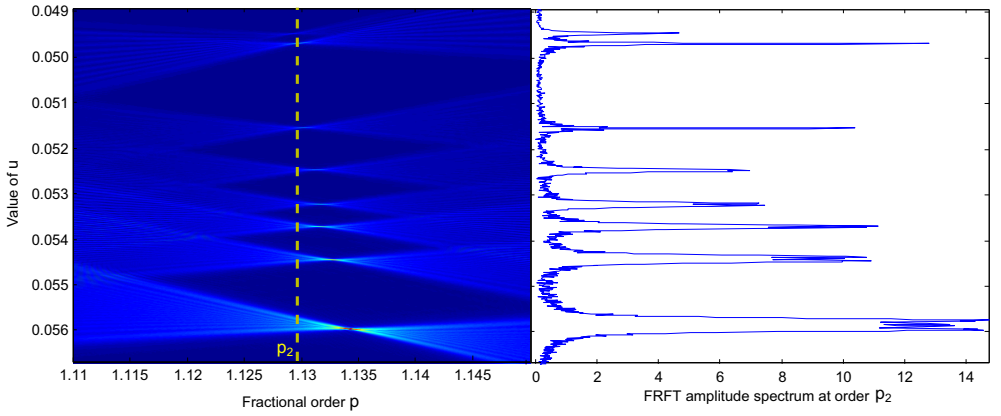

(b) The multipaths undergo different scaling changes

Fig. 2. The FrFT amplitude spectrums of the overlapped received signal at specific fractional orders. The left parts of (a) and (b) show the FrFT results in the u-p plane, and the right parts are the FrFT amplitude spectrums at the fractional order $p = p_1$ and $p = p_2$, respectively.

forms an impulse at the ORA, searching for the ORA is equivalent to scanning the fractional Fourier amplitude spectrum for the maximum value. We use a coarse-to-fine scanning mode proposed in [16], and revise it in Algorithm 1 as needed. As proposed in [23], the fast digital FrFT algorithm could reduce any fractional order to a general interval $(0.5, 1.5)$, so it is employed here to calculate the FrFT of the sampled signal. Like FFT, this fast algorithm gives samples of the continuous time FrFT of a signal in terms of the same amount of samples of the original signal.

Assuming the transmitted LFM signal $s(t)$ has N samples under the sampling rate f_s, then the time interval is $\Delta t = 1/f_s$. Under such discretization, according to the fast digital FrFT [23], the lengths of both time and frequency intervals are set to the dimensionless quantity $\sqrt{Tf_s}$. Dividing the time dimension by $\sqrt{T/f_s}$ and multiplying the frequency dimension by $\sqrt{T/f_s}$, the signal can be represented with Tf_s samples in new coordinates. Thus, the modulation slope of the sampled LFM signal changes to

$$k_d = \frac{(f_1 - f_0)\sqrt{T/f_s}}{T/\sqrt{T/f_s}} = k\frac{N\Delta t}{f_s} = \frac{kN}{f_s^2} \tag{12}$$

Replacing k with k_d in (11), we have the scale factor, estimated by Algorithm 1 using the digital FrFT, as

$$\hat{\alpha} = \sqrt{-\frac{f_s^2}{kN}\cot\phi'^{\star}}. \tag{13}$$

The computational complexity of the scanning is linear with the iteration times γ_r, which controls the precision of the scanning to fractional order p. Since the fast discrete FrFT requires $O(N\log N)$ computation [23], the total scanning complexity will be $O(N_{\mathrm{FrFT}}N\log N)$, where N_{FrFT} is the total number of FrFT times in the scanning, defined in equation (7) of [16] and equal to $11(\gamma_r + 1)$ in this paper. Through simulation, we find that a good scanning performance can be achieved if γ_r is set larger than $\log k$.

B. Estimation of the Delay and Amplitude Parameters

For delay estimation, we utilize the pulse compression of LFM signals in the time domain, i.e., its excellent self-correlation characteristic. If the received signal is an attenuated and time-shifted copy of the transmitted signal, the cross-correlation between them will form a narrow pulse, and therefore increases the delay resolution as well as the signal to noise ratio (SNR).

From [24] (Equation 2.118, Chapter 2.1.2.3), we know that the autocorrelation function of a bandpass LFM signal is

This article has been accepted for publication in a future issue of this journal, but has not been fully edited. Content may change prior to final publication. Citation information: DOI 10.1109/TSP.2016.2582466, IEEE Transactions on Signal Processing

similar to a sinc function. Its maximum is reached at $\tau = 0$. Hence, once the scale factor of the received signal is estimated, then the time delay τ and amplitude A can be estimated through searching for the peak of the cross-correlation between $r(t)$ and $s_{\widehat{\alpha}}(t)$, where $s_{\widehat{\alpha}}(t) = s(\hat{\alpha}t)$ is the resampled $s(t)$ with $\hat{\alpha}$ as the resampling factor, i.e.

$$\widehat{\tau} = \arg\max_{\tau} \left\{ \int_{-\infty}^{\infty} r(t) s_{\widehat{\alpha}}^{*}(t-\tau) dt \right\} \tag{14}$$

and

$$\widehat{A} = \frac{\int_{-\infty}^{\infty} r(t) s_{\widehat{\alpha}}^{*}(t-\widehat{\tau}) dt}{\int_{-\infty}^{\infty} \|s_{\widehat{\alpha}}(t)\|^2 dt} \tag{15}$$

IV. FrFT-based Parameter Estimation for MSML Channels

Parameter estimation is relatively simple for the single path case. However, it can be much more complicated for MSML channels. As stated in Section II, the received signal could be overlapped by several multipath components with different scales and delays. In [12], it assumes that the components undergo one identical scaling change. In other words, the multipath signals share the same ORA, and all of them will form impulses in the FrFT domain with a specific fractional order so as to be discernible, as shown in Fig.2(a). Here, we scan the FrFT rotation angle of the received signal and draw the FrFT results in the u-p plane. It can be seen that for each multicomponent, the FrFT result forms an "X"-shape belt across the fractional order axis, and peaks at the cross of the "X" belt. In Fig.2(a), the crosses of the "X" belts are all in a straight line $p = p_1$, so the multicomponents can be discerned from the FrFT spectrum at order p_1.

The situation becomes complicated when the multipath components have different scales. Considering a channel with 8 paths of nonzero amplitudes and different scales, the received signal's FrFT with a certain range of fractional orders is shown in Fig.2(b). It can be seen that the crosses of the "X" belts are no longer in a straight line. Furthermore, let us observe the component with the second lowest energy, i.e., the second "X" belt from top to bottom in the left part of Fig.2(b), whose optimal fractional order is denoted as p_2. The FrFT amplitude at order p_2 is shown in the right part of Fig.2(b). It can be seen that the second component forms an impulse in the FrFT amplitude spectrum; while the FrFT of the component with highest energy, the last "X" belt from top to bottom in the left part of Fig.2(b), is still larger than the impulse peak of the second component in a certain range of u value. Thus, it is difficult to determine ORA for the second component. That is to say, the strong multicomponents can interfere the detection and parameter estimation of the weak ones.

Note that, for an identical multipath signal, its u-p planar graph resembles its graph in the wideband ambiguity function plane. In previous research, the MP algorithm [9] is used to decompose the multipath signals in the wideband ambiguity function plane, and provide path parameter estimates in terms of delays, scale factors and amplitudes. However, a complete signal dictionary is needed for MP algorithm. The atoms of the dictionary should cover all possible combinations of the discrete delays and scales in (32) or (33), given in Appendix A. Thus, higher scale and delay resolutions require more atoms with longer sampling lengths, which enlarge the size of signal dictionary and increase computation cost.

Next, inspired by the thought of MP algorithm, we propose an iterative parameter estimation algorithm, which separates the multipath components one by one according to the energy level. At each iteration, more specifically, the scale factor, delay and amplitude of each dominant component are estimated on the principle given in the last section, with a sub-iteration contained to adjust the optimal fractional order. Once the parameters of a multipath are precisely estimated, the corresponding component will be separated from the received signal through eliminating the resampled, delayed and attenuated version of the original probe signal.

A. Iterative Method with Fractional Order Adjusting

Specifically, suppose that the i-th path signal has the largest amplitude A_i, the overlapped received signal can be given as

$$r(t) = A_i s_i(t) + \sum_{l=1, l\neq i}^{L} A_l s_l(t) + w(t), \tag{16}$$

where $s_l(t) = s\left(\alpha_l(t-\tau_l)\right), l = 1, \cdots, L$, denotes the l-th path signal. Denote T_{is}, T_{ie} as the starting time and ending time of the i-th path signal, respectively. $w(t)$ is the additive noise. On one hand, according to the linearity, the p-order FrFT of $r(t)$ in (16) within a time section $[T_s, T_e]$ is

$$\begin{aligned} F^p r = R_\phi(u) \;=\; & A_i S_{i,\phi}(u) + \sum_{l=1, l\neq i}^{L} A_l S_{l,\phi}(u) + W_\phi(u), \\ & u \in [|\csc\phi| f_L, |\csc\phi| f_H], \end{aligned} \tag{17}$$

where f_L and f_H are the lowest frequency and highest frequency of the L components within $[T_s, T_e]$. It is proved in Appendix B that if $[T_s, T_e]$ contains $[T_{is}, T_{ie}]$, the FrFT of $r(t)$ with rotation angle $\phi_i^\star$, the ORA of $s_i(t)$, becomes

$$\begin{aligned} R_{\phi_i^\star}(u) \;=\; & A_i C_i(u) \mathrm{sinc}\big(b_i\left(u - u_i^\star\right)\big) + \sum_{l=1, l\neq i}^{L} A_l S_{l,\phi_i^\star}(u) \\ & + W_{\phi_i^\star}(u), \quad u \in [|\csc\phi_i^\star| f_L, |\csc\phi_i^\star| f_H], \end{aligned} \tag{18}$$

$$\langle r, s_{\alpha_i}\rangle(\tau) = A_i \int_{-\infty}^{\infty} s_i(t) s_{\alpha_i}^{*}(t-\tau) dt + \sum_{l=1, l\neq i}^{L} A_l \int_{-\infty}^{\infty} s_l(t) s_{\alpha_i}^{*}(t-\tau) dt + \int_{-\infty}^{\infty} w(t) s_{\alpha_i}^{*}(t-\tau) dt \tag{19}$$

$$A_i \int_{-\infty}^{\infty} s_i(t) s_{\alpha_i}^{*}(t-\tau) dt = \frac{1}{\alpha_i} A_i T \Lambda\left(\frac{\alpha_i(\tau-\tau_i)}{T}\right) \mathrm{sinc}\left[\pi k \alpha_i T(\tau-\tau_i) \Lambda\left(\frac{\alpha_i(\tau-\tau_i)}{T}\right)\right] e^{j2\pi\alpha_i f_0(\tau-\tau_i)} \tag{20}$$

This article has been accepted for publication in a future issue of this journal, but has not been fully edited. Content may change prior to final publication. Citation information: DOI 10.1109/TSP.2016.2582466, IEEE Transactions on Signal Processing

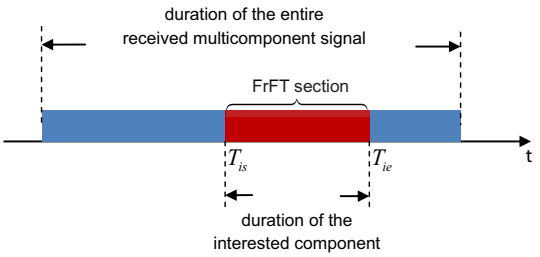

Fig. 3. Signal section for FrFT in each iteration of Algorithm 2. The algorithm starts by operating FrFT on the entire multicomponent signal, and finally shrinks and positions the FrFT section to fit the interested component.

where $C_i(u)$, b_i and $u_i^\star$ are given in Appendix B. It is also proved in Appendix B that the energy of $s_i(t)$ can be retained and the absolute value of $R_{\phi_i^\star}(u)$ maximizes at $u_i^\star$ since the first term of the right-hand side of (18) tends to be a narrow pulse. The second term of the right-hand side of (18) is considered as the interference caused by the $\phi_i^\star$-rotated FrFT of the weak components, and the third term is noise.

On the other hand, denoting $s_{\alpha_i}(t) = s(\alpha_i t)$ as the resampled version of $s(t)$ with α_i as the resampling factor, the cross correlation between $r(t)$ and $s_{\alpha_i}(t)$ can be written as (19), shown at the bottom of last page. Being similar to [24], the first term of the right-hand side of (19) can be expressed as (20), shown at the bottom of last page, where $\Lambda(t)$ is the triangle function defined on $[0, 1]$, increasing from 0 to 1 linearly on $[0, \frac{1}{2}]$, and decreasing from 1 to 0 linearly on $[\frac{1}{2}, 1]$. The second term of the right-hand side of (19) is considered as the interference caused by the weak components. The maximum of $\langle r, s_{\alpha_i}\rangle(\tau)$ is reached at $\tau = \tau_i$.

Hence, if the current most dominant component $\hat{A}_i s_i(t)$ is precisely separated from the received signal, the compressed pulses, i.e. the first terms of (18) and (19), will be removed. There will be no interference involving $s_i(t)$ left for the separation of the next strongest component. The most important work is the parameter estimation for the strongest component in the residual received signal.

According to the above analysis, a novel parameter estimation scheme is proposed, given as Algorithm 2. The proposed algorithm proceeds in an iterative manner and returns the parameter estimates of the most dominant component successively. For each component, the parameter estimation is a planar searching process in the scale-delay plane. A sub-iteration, i.e., steps 2-5, is contained to adjust the optimal fractional order for each multicomponent.

Like the single-path case, the pulse compression of LFM signals, both in time domain and FrFT domain, is used. For each iteration, the scale factor is estimated by scanning the FrFT of the sectioned signal and seeking the ORA, while the delay is estimated via searching for the peak of the cross-correlation between the received signal and the resampled training signal. Nevertheless, unlike the single-path case, here the scale factor estimation and the delay estimation are jointly conducted. The width and position of the FrFT window will dynamically change until the fractional order, or equivalently the estimated scale factor, is stabilized. In this way, the starting time and length of the current component can be determined very precisely, illustrated as Fig.3. Once the parameters are estimated, the current component will be separated by eliminating the resampled, delayed and attenuated version of the probe signal in time domain, as shown in step 7.

Algorithm 2 Iterative parameter estimation algorithm with fractional order adjusting

Input:

transmitted LFM signal vector $\mathbf{s}_{N\times 1}$ and its modulation slope k; received signal vector $\mathbf{r}_{N_r\times 1}$; a predicted SNR; a small enough positive ε;

Initialization:

Set the residual signal vector $\mathbf{r}_e = \mathbf{r}$, maximum number of iterations, L; iteration index $i = 1$;

Iteration:

1: Using Algorithm 1, obtain the i-th ORA $\phi_i^\star = p_i^\star \pi/2$ by scanning the FrFT of $\mathbf{r}_e$, and compute the i-th scale estimate

$$\widehat{\alpha}_i = \sqrt{-\frac{f_s^2}{kN_r}\cot\phi_i^\star}; \tag{21}$$

2: Resample $\mathbf{s}$ with scale $\widehat{\alpha}_i$ to obtain $\mathbf{s}_i$ whose length is $N_i = \lceil \widehat{\alpha}_i N \rceil$;

3: Operate a cross correlation between $\mathbf{s}_i$ and $\mathbf{r}_e$, and find the delay index as

$$d = \max_n \left| \sum_m \mathbf{r}_e[m]\mathbf{s}_i^*[m+n] \right|; \tag{22}$$

4: Rescan the FrFT of $\mathbf{r}_e[d : d + N_i - 1]$ and obtain a new ORA and a new scale estimate $\widehat{\alpha}_i'$;

$$\widehat{\alpha}_i' = \sqrt{-\frac{f_s^2}{kN_i}\cot\phi_i^\star}; \tag{23}$$

5: IF $|\widehat{\alpha}_i' - \widehat{\alpha}_i| > \varepsilon$, let $\widehat{\alpha}_i = \widehat{\alpha}_i'$ and repeat step 2-4; ELSE go to step 6.

6: Compute the estimates of the i-th multipath delay and complex amplitude by

$$\widehat{\tau}_i = d/f_s, \quad \widehat{A}_i = \sum_m \mathbf{r}_e[m]\mathbf{s}_i^*[m+d]/\|\mathbf{s}_i\|_2^2; \tag{24}$$

7: Update residual signal

$$\mathbf{r}_e[d : d + N_i - 1] \leftarrow \mathbf{r}_e[d : d + N_i - 1] - \widehat{A}_i \mathbf{s}_i;$$

8: IF $i = L$ or the ratio $\|\mathbf{r} - \mathbf{r}_e\|_2^2/\|\mathbf{r}_e\|_2^2$ reaches the predicted SNR, stop the iteration; ELSE, set $i = i + 1$ and go to step 1;

Output:

The estimated channel parameters $\{\widehat{\mathrm{A}}_i, \widehat{\alpha}_i, \widehat{\tau}_i\}_{i=1}^L$.

B. Comparison with Other Methods

Some other methods, which use LFM signals and FrFT, have already been mentioned in Section I. In order to make a better distinction between them and the proposed method, a comparison of these methods is listed in Table.I.

This article has been accepted for publication in a future issue of this journal, but has not been fully edited. Content may change prior to final publication. Citation information: DOI 10.1109/TSP.2016.2582466, IEEE Transactions on Signal Processing

It can been that the Problem 1 in Table.I, the relationship between the discrete FrFT section of the sampled received signal and the time duration of the individual multipath signal, is almost neglected in the literatures. In fact, the exact length and position of the discrete FrFT section is hard to be determined, since the lengths and starting times of the scaled and delayed multicomponents are unknown and different with each other. In Algorithm 2, we fully consider this problem. In steps 3 and 4, the FrFT section can adaptively change and shrink to the actual time duration of the interested multipath signal, see Fig.3. In [11] and [14], the FrFT section length is selected as the length of the complete received signal. However, although it can be guaranteed that the duration of each multicomponent is contained in FrFT section, larger FrFT section does not suggest more accurate estimates. According to the FrFT definition, the transformation kernel is a set of chirp bases. In discrete processing, due to the discretization error, longer bases may produce a deviation when seeking the ORA and estimate the scale factor. Such deviation will also influence the estimation accuracy of the delay and amplitude parameters. In Section V, we will demonstrate that this deviation caused by the length of discrete FrFT does exist.

The ST-FrFT domain filter, which sections the observed signal by short-time windows [18] [22], can be used to shrink the transform section. But the width of short-time window should be determined in advance to ensure the individual component can be contained. In addition, the ST-FrFT is time-consuming. According to [18], the computational complexity of the ST-FrFT is $O(N^2 \log N)$; while the major computation of Algorithm 2 is spent on FrFT scanning, i.e. the Algorithm 1, whose computational complexity is $O(N_{\mathrm{FrFT}} N \log N)$.

Different from what was done in [11], [14], [17] and [18], moreover, we separate the multicomponents in time domain rather than in the FrFT domain. Although the FrFT/ST-FrFT domain filters used in those references can extract the scale feature of the original signal, they do not perform well in separating the multicomponents from the overlapping LFM signal. It is because that there may be some energy loss at the edge of the filtering window [18]. By contrast, the proposed method separates the strongest component in each iteration by eliminating the resampled and delayed version of the training signal from the residual signal, i.e. Step 7 in Algorithm 2. One by one, the overlapped multicomponents are separated in time domain and the time aliasing is cancelled. The separation can perform very well if the parameters are accurately estimated.

TABLE I
COMPARISON OF PARAMETER ESTIMATION METHODS USING LFM SIGNALS

Ref.	Multi-scale	Multi-lag	Signal Separation	P1[1]	P2[2]
[11]	No	Yes	FrFT domain filter	No	-
[12]	No	Yes	None	No	No
[13]	No	No	None	No	Yes
[14]	Yes	No	FrFT domain filter	No	Yes
[15]	Yes	Yes	None	No	Yes
[16]	Yes	No	None	No	Yes
	No	Yes			
[17]	No	No	FrFT domain filter	Yes	-
[18]	Yes	Yes	ST-FrFT domain filter	Partly	No
[9]	Yes	Yes	MP decomposition	-	Yes
Ours	Yes	Yes	Time domain aliasing cancellation	Yes	Yes

[1] Problem 1: Is the relationship, between the discrete FrFT section of the sampled received signal and the time duration of the individual multipath signal, considered?
[2] Problem 2: Is it unnecessary to know the scale factors of the multicomponents beforehand?

V. SIMULATION RESULTS

In this section, the proposed parameter estimation method is evaluated by computer simulation. Firstly, we demonstrate that the fractional order adjusting process, i.e. steps 2-5 of Algorithm 2, can improve estimation accuracy. Secondly, we evaluate the performance of the time-domain multicomponent separation. Finally, the performance of entire proposed method is evaluated. Note that, the performance of the proposed method in the time-varying underwater acoustic channel with a moving receiver is evaluated in [25], where the channel impulse response is generated by BELLHOP, a well-known acoustic pressure fields predicting program for ocean environments following the ray tracing model.

The parameters of the transmitted LFM signal in the simulation are assumed as follows. The bandwidth and time duration are set to be $B = 10$kHz and $T = 50$ms, thus the modulation slope is $k = B/T = 2 \times 10^5$. The starting frequency, stopping frequency and initial phase are $f_0 = 5$kHz, $f_1 = 15$kHz, and $\varphi_0 = 0$, respectively. Unless otherwise specified, the sampling rate f_s is set as 8 times of the signal bandwidth B (=$f_1 - f_0$).

A. Adjusting Performance of the Optimal Fractional Order

According to Algorithm 2, the scale factor and delay of each component are jointly estimated by iteratively adjusting the estimate of ORA. In fact, the sub-iteration, steps 2-5, ensures that the FrFT window width can shrink from the length of the complete received signal to the length of the specific component within a few loops.

Without considering the noise, let us assume that a single-path signal is received, which is scaled by $\alpha = 1.01$. We fill in front of the sampled signal with zeros, the number of which indicates the time delay. Suppose the length of the scaled signal vector is N_i and the zero-padding number is N_0, we have the complete length of the received signal as $N_r = N_i + N_0$. In Section IV-A, we have mentioned that larger FrFT section does not mean more accurate estimates. It can be illustrated by setting N_r as the FrFT section length, and changing the zero-padding number N_0.

The relationship between the fractional order error and the zero-padding number is drawn in Fig.4. The line in blue color represents the error of fractional order estimate using the N_r-length FrFT length, i.e. without order adjusting, while the line in red color represents the error using the order adjusting. The error is calculated as $|\widehat{p} - p^\star|$, where $\widehat{p}$ and $p^\star$ denotes the fractional order estimate and the optimal fractional order of the scaled signal, respectively. It can be seen that the order estimate error without adjusting increases, with small fluctuations, as the zero-padding number increases. By

This article has been accepted for publication in a future issue of this journal, but has not been fully edited. Content may change prior to final publication. Citation information: DOI 10.1109/TSP.2016.2582466, IEEE Transactions on Signal Processing

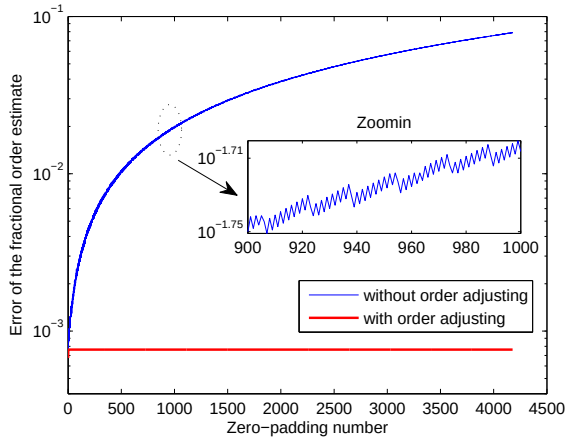

Fig. 4. The error of the fractional order estimate versus the zero-padding number. The duration length of the scaled signal is $N_i = 4040$, and the zero-padding number N_0 changes from 0 to 4200.

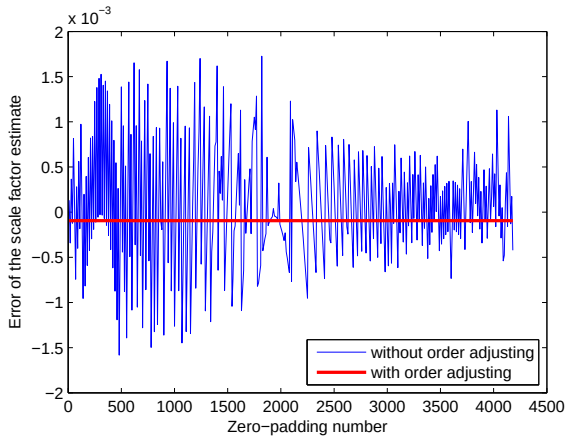

Fig. 5. The error of the scale factor estimate versus the zero-padding number.

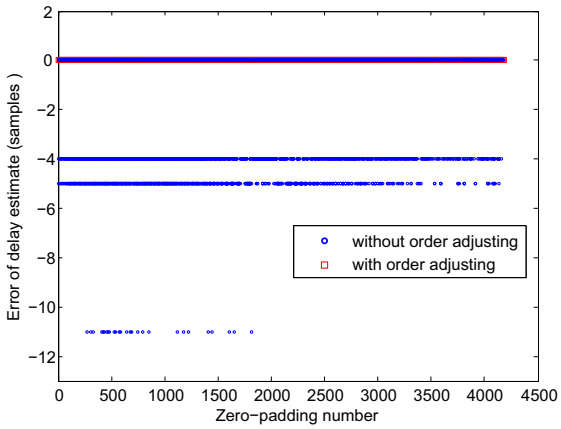

Fig. 6. The error of the estimated delay samples versus the zero-padding number.

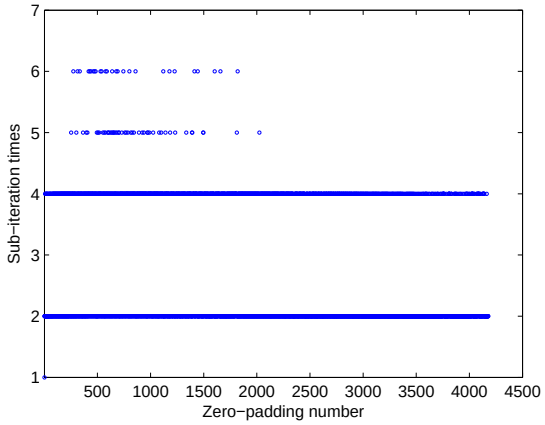

Fig. 7. The sub-iteration times versus the zero-padding number.

contrast, the order adjusting process can control the error very nicely.

Since the modulation slope is large and the scale factor is close to 1, we can expect the ORA is close to π from (10). Further, it is expectable that the estimation performance of the fractional order has sensitive influence on that of the scale factor. The errors of the scale factor, for both with and without order adjusting, are plotted as Fig.5. The fluctuating error for the estimate without order adjusting is caused by the fluctuations in Fig.4, which is in accordance with (21). By contrast, the fractional order adjusting process is able to stabilize the error at an extremely low level.

The estimation error of scale factor may cause a deviation of a few samples for the peak searching of the cross correlation in (22), hence lead to an inaccurate delay estimate. The deviations of the samples, versus the zero-padding number, are drawn in Fig.6. If order adjusting is not used, there will be a deviation on the delay estimate, up to 11 samples. Such error can be removed by using order adjusting.

Finally, the number of order adjusting loops should be concerned, since more loops needs more calculation amount. As shown in Fig.7, two or four order adjusting loops are required for most zero-padding numbers, and up to six loops are required for a few zero-padding numbers.

B. Performance of Multicomponent Separation

From Table.I, we can see many existing works use FrFT domain filter or ST-FrFT domain filter to separate the multi-component LFM signals. Rectangular windows or Gaussian windows are used to extract the interested component and the retrieved signal is obtained via inverse FrFT/ST-FrFT. However, the retrieved signal slightly differs from the actual corresponding component, because the sudden change of the window edges results in some energy loss at the edges of the pulse in the FrFT spectrum. In this subsection, the performance of the proposed time-domain multicomponent separation method in Algorithm 2 is evaluated and compared with the performance of FrFT domain filter and ST-FrFT domain filter.

To put it simple, we consider a two-path channel and the received signal is expressed as

$$r(t) = A_1 s(\alpha_1(t-\tau_1)) + A_2 s(\alpha_2(t-\tau_2)) + w(t)$$

where $A_1 = 1$, $A_2 = 0.9$, $\alpha_1 = 1$, $\alpha_2 = 1.01$, $\tau_1 = 0$ms, and $\tau_2 = 3.75$ms in the simulation. Here the scale factors

This article has been accepted for publication in a future issue of this journal, but has not been fully edited. Content may change prior to final publication. Citation information: DOI 10.1109/TSP.2016.2582466, IEEE Transactions on Signal Processing

are assumed known by the FrFT domain filter and ST-FrFT domain filter, see Table.I-P2. In addition, considering the effect of the sampling rate to the accuracy of the scale factor estimation, we set $f_s = 2B, 4B$ and $8B$ separately in the simulation.

The residual signal energy rate, $\|\mathbf{r}_e\|^2/\|\mathbf{r}\|^2$, is selected as the indicator to assess the separation performance, and the results are shown in Fig.8. Obviously, the proposed time-domain separation performs better than the FrFT domain separations. When the sampling rate reaches $f_s = 8B$, the time-domain separation is almost ideal.

C. Performance of Entire Parameter Estimation

In this part, we evaluate the performance of the entire proposed parameter estimation algorithm, and compare it with the MP-based method [9].

To do so, we construct two signal dictionaries, which correspond to the two virtual representations of the delay-scale spreading function (DSSF), given in (32) and (33) of Appendix A. The dictionaries are composed of atoms which are scale-delay versions of the original LFM signal. The atoms of the first are uniformly sampled on scale factor with the sampling interval $\Delta\alpha = 0.001$, while the atoms of the second are geometrically sampled on scale factor with the basic factor $\alpha_0 = 1.001$. To distinguish the MP-based methods that use different dictionaries in the simulation, we call the method that using the former dictionary scale-uniform-sampling MP (SUS-MP) algorithm and the one using the latter dictionary scale-geometrical-sampling MP (SGS-MP) algorithm.

To begin with, we hypothesize an original sparse MSML UWA channel for the simulation, and then we make the following assumptions:

1) only 8 multipaths are dominant in energy, whose amplitudes follow uniformly distribution;

2) all the multipaths are time-compressed and the scale factors are uniformly distributed within $\alpha \in [1, 1.02]$, with an accuracy to three decimal places (Note that the maximum scale 1.02 corresponds to a relative velocity about 30 knots, which is relatively high for underwater movement);

3) all the multipaths arrive at the receiver within one signal duration T (significantly overlapping case), and the delays follow uniformly distribution.

The channel shown in Fig.2(b) is just an example for reference.

Note that the proposed method applies the path-based channel model, (2), and the MP-based method applies the DSSF's virtual representation model, (34) of Appendix A. On account of the model difference, the output of Algorithm 2 should be modified into the DSSF matrix form so as to compare their the estimation accuracy fairly. With the above assumptions, a sparse DSSF matrix $\mathbf{H}_{M\times N}$ can be obtained for the simulation. Combining the normalization factor, the (m,n)-th element is $\mathbf{H}[m,n] = \alpha_m^{\frac{1}{2}}\mathfrak{h}_{m,n}$. The path-based scale factors, delays, and amplitudes can be modified by

$$\begin{cases} \alpha_m = 1 + (m-1)/1000 \\ \tau_n = (n-1)/f_s \\ A_{m,n} = \mathbf{H}[m,n] = \alpha_m^{\frac{1}{2}}\mathfrak{h}_{m,n} \end{cases}, \quad \begin{array}{c} \text{for } m = 1, ..., M, \\ n = 1, ..., N. \end{array} \tag{25}$$

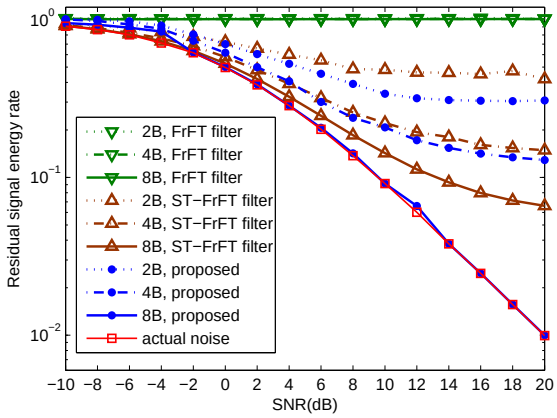

Fig. 8. Multicomponent LFM signal separation performance: residual signal energy rate versus SNR

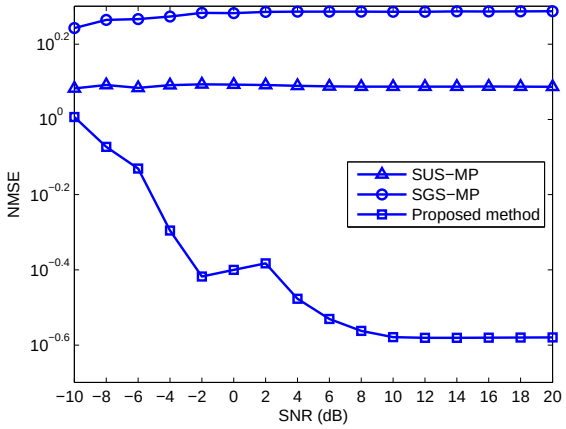

Fig. 9. NMSEs of the DSSF estimates versus SNR

1) Performance Comparison of the DSSF estimations: The DSSF estimation is actually a process of estimating the parameters α, τ and A. Thus, the estimation accuracy of each parameter will have impact on the overall performance of the DSSF estimation. We mainly use the following normalized mean squared error (NMSE) as the performance indicator of the estimation,

$$\mathrm{NMSE}_{\mathrm{DSSF}} = \frac{\int_{-\infty}^{\infty}\int_{-\infty}^{\infty}\left|\widehat{H}(\alpha,\tau) - H(\alpha,\tau)\right|^2 d\tau d\alpha}{\int_{-\infty}^{\infty}\int_{-\infty}^{\infty}\left|H(\alpha,\tau)\right|^2 d\tau d\alpha} \tag{26}$$

where $H(\alpha,\tau) = \alpha^{\frac{1}{2}}h(\alpha,\tau)$ is the normalized DSSF, and $\widehat{H}$ is the estimate. Since we keep three decimal places for the scale factor and $\alpha_0^{20} \approx 1.02$, both of the MP-based algorithms obtain 21 samples of the scale factor within the range $[1, 1.02]$. In addition, by using the parameters $\widehat{\alpha}$, $\widehat{\tau}$, and $\widehat{A}$ estimated by Algorithm 2, we can rebuild the discrete DSSF matrix from (25). The discrete computation of (26) is expressed as

$$\mathrm{NMSE}_{\mathrm{DSSF}} = \frac{\sum_m\sum_n\left|\widehat{\mathbf{H}}[m,n] - \mathbf{H}[m,n]\right|^2}{\sum_m\sum_n\left|\mathbf{H}[m,n]\right|^2} \tag{27}$$

This article has been accepted for publication in a future issue of this journal, but has not been fully edited. Content may change prior to final publication. Citation information: DOI 10.1109/TSP.2016.2582466, IEEE Transactions on Signal Processing

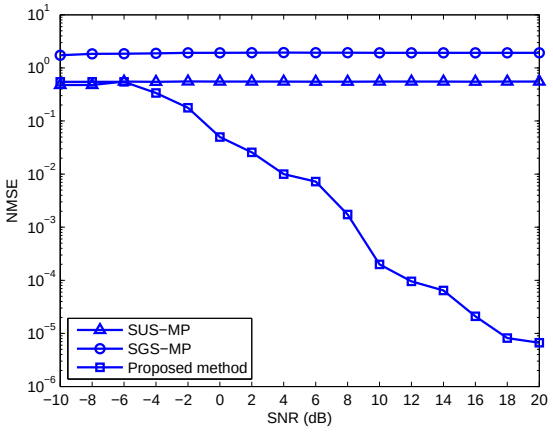

Fig. 10. NMSEs of the estimated power delay profile (PDP) versus SNR

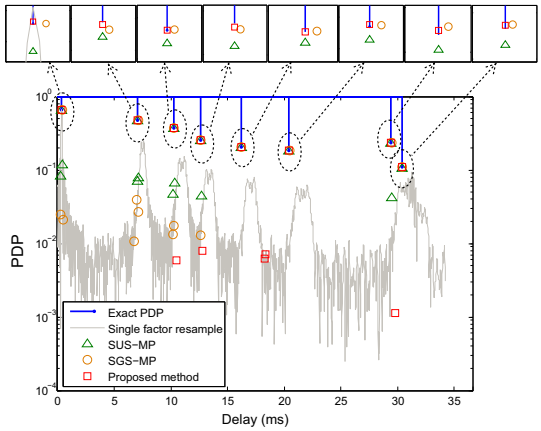

Fig. 11. Estimated PDP at SNR=20dB (one trial). The dominant delay areas are zoomed in on top of the figure. The proposed method can approach the exact PDP at the dominant delay positions. The SUS-MP and SGS-MP, however, show relatively larger deviations.

where $\widehat{\mathbf{H}}[m,n] = \widehat{\alpha}_m^{\frac{1}{2}} \widehat{\mathfrak{h}}_{m,n}$ denotes the discrete DSSF estimate for all the simulated algorithms.

The NMSE of the estimated DSSFs using SUS-MP, SGS-MP and the proposed method versus SNR is drawn in Fig.9. It can be seen that the performance of the proposed estimation method is significantly better than the MP-based estimation methods.

2) Performance Comparison of the Power Delay Profile: In many cases, we care more about the estimation accuracy of power delay profile (PDP) of the channel since PDP carries important information, such as the path intensity and distance between the transmitter and the receiver or between the detector and the target. The PDP of the channel can be obtained by stacking up the scale dimension of the DSSF. The NMSE of the PDP estimate can be expressed as

$$\mathrm{NMSE}_{\mathrm{PDP}} = \frac{\sum_n \left| \sum_m \widehat{\mathbf{H}}[m,n] - \sum_m \mathbf{H}[m,n] \right|^2}{\sum_n \left| \sum_m \mathbf{H}[m,n] \right|^2} \tag{28}$$

Fig.10 shows the NMSEs of the estimated PDP versus SNR. Note that the performance of the proposed method gaps away from the SUS-MP method after the SNR exceeds -6dB. The PDP estimates in once trial at SNR=20dB is shown in Fig.11. The output of the matched filter with a single resample factor [10], corresponding to the scale of the most dominant path, is also drawn (in gray line) to show the LFM signal's wideband auto-ambiguity function influence on the delay detection. We can see that the proposed method locates the delays of the dominant multicomponents very well. The MP-based method, however, shows relatively larger deviations and may leak the energy to some other positions along the delay axis.

3) Performance Comparison of the Scale Factor Estimations: Like the way to get PDP, we can obtain the power scale profile by stacking up the delay dimension of the DSSF. The NMSE of the power scale profile estimate is defined as

$$\mathrm{NMSE}_{\mathrm{PSP}} = \frac{\sum_m \left| \sum_n \widehat{\mathbf{H}}[m,n] - \sum_n \mathbf{H}[m,n] \right|^2}{\sum_m \left| \sum_n \mathbf{H}[m,n] \right|^2} \tag{29}$$

The NMSEs of the estimated power scale profile versus SNR is given as Fig.12. The proposed method performs much better than the MP-based method, and gaps away from the SUS-MP method after the SNR exceeds -8dB. Nevertheless, the performance of power scale profile estimation does not entirely represent the accuracy of the scale estimates. We turn to investigate the NMSEs of the scale factor estimates of the dominant multipaths, i.e.

$$\mathrm{NMSE}_{\mathrm{scale}} = \frac{\sum_{l=1}^{L} |\widehat{\alpha}_l - \alpha_l|^2}{\sum_{l=1}^{L} |\alpha_l|^2} \tag{30}$$

and show the results in Fig.13. The proposed method obtains more accurate scale estimates than MP-based method when SNR surpasses -2dB.

Note that the performance of MP-based method does not become better as the SNR increases, i.e. their NMSEs have no evident downtrend in Fig.9, 10, 12 and 13. Instead, the performance slightly goes worse. Such result owes to the poor scale resolution of LFM signal in the delay-scale domain, so the MP-based method might always obtain an inaccurate estimate of the scale factor, which causally results in an inaccurate delay estimate. Moreover, once the estimated parameter of the first iteration is deviated, the latter iterations might compensate for it and cause greater deviation. In contrast, the proposed method converts the discrimination of the scale into more moderate discrimination of the optimal fractional order. Hence, the proposed method can obtain much more accurate parameter estimates.

VI. Conclusion

In this paper, the wideband UWA channels are modeled as MSML channels to depict the multipath structural compo-

This article has been accepted for publication in a future issue of this journal, but has not been fully edited. Content may change prior to final publication. Citation information: DOI 10.1109/TSP.2016.2582466, IEEE Transactions on Signal Processing

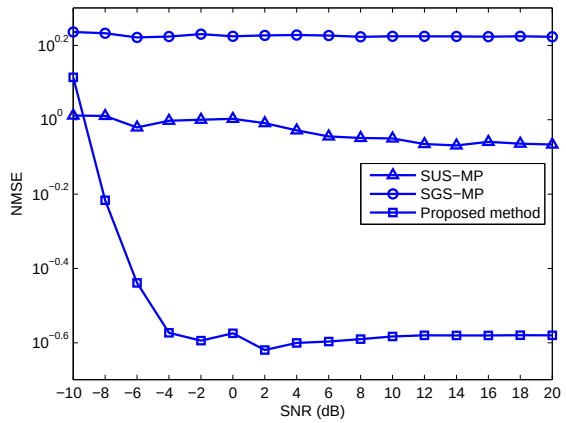

Fig. 12. NMSEs of the estimated power scale profile versus SNR

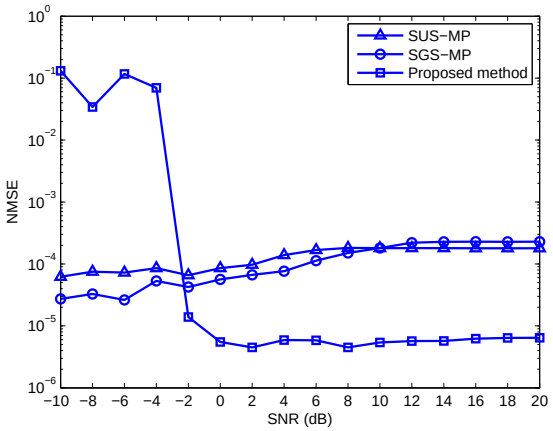

Fig. 13. NMSEs of the scale factor estimates of the dominant multipaths versus SNR

sition. The Doppler scale factors and time delays are path-based, and can be differentiated with each other. The parameter estimation for such channels is investigated with some considerations for practical digital processing. On the basis of existing research, a more accurate and efficient estimation method is proposed. The LFM signal is transmitted as the training signal. In the single-path case, we illustrate that the Doppler scaling change is equivalent to the rotation of ORA in FrFT domain. Thus the scale factor can be estimated by searching for the ORA, and the delay can be estimated through a cross-correlation. The estimation process utilizes the pulse compression in both time domain and FrFT domain. For the multipath case, the received multicomponents are decomposed in order of descending energy. For each component, the parameters are jointly and precisely estimated via an iterative planar searching process in the scale-delay plane. A sub-iteration, which adjusts the optimal fractional order, is also contained to achieve higher estimation precision. Then the interested component can be separated from the entire received signal. Simulation results prove that the order-adjusting process of the proposed method can effectively improve estimation accuracy. With more accurate parameter estimates, the time-domain separation is superior to FrFT/ST-FrFT domain filters. Finally, the performance of the proposed method surpasses the MP-based method, since it offers a finer and more flexible scale resolution.

Appendix A
Delay-Scale Domain System Modle

The delay-scale spreading function (DSSF), denoted as $h(\alpha,\tau)$, is a continuous function which takes the temporal scaling α (caused by Doppler effect) and delay τ as variables [4], [7], [9], [21], [26]. At the receiver, the received signal $r(t)$ can be expressed as

$$r(t)=\int_{-\infty}^{\infty}\int_{-\infty}^{\infty}h(\alpha,\tau)\alpha^{\frac{1}{2}}s\left(\alpha\left(t-\tau\right)\right)d\tau d\alpha \tag{31}$$

where $\alpha^{\frac{1}{2}}$ is a normalization factor. Equation (31) can represent any linear time-varying channel, and it is more suitable for the wideband UWA channels [4].

The DSSF of UWA channels can be discretized through sampling the delay-scale plane. In [27], a *virtual representation* of a multipath channel is used to provide a discretized approximation of its time-varying frequency response by uniformly sampling the angle-delay-Doppler space. The virtual representation will be an accurate approximation if the discretion of scale and delay has fine enough resolution. In this paper, we adopt such virtual representation and investigate two sampling modes.

Firstly, similar to [27], a discrete DSSF can be obtained by uniformly/arithmetically sampling the delay-scale plane at regular intervals. Specifically, assuming $h\left(\alpha,\tau\right)=0,\ \forall(\alpha,\tau)\notin[\alpha_{\min},\alpha_{\max}]\times[0,\tau_{\max}]$, where $\alpha_{\min}$, $\alpha_{\max}$ and $\tau_{\max}$ denote the lower bound, upper bound of the scale changing and the maximum delay of the channel, respectively, the virtual representation of the DSSF is given by

$$\widetilde{h}_U\left(\alpha,\tau\right)=\sum_{m=1}^{\mathcal{M}}\sum_{n=0}^{\mathcal{N}}\mathfrak{h}_{m,n}^{U}\delta\left(\alpha-\alpha_m\right)\delta\left(\tau-\tau_n\right) \tag{32}$$

where $\alpha_m=\alpha_{\min}+m\Delta\alpha$, $\tau_n=n\Delta\tau$, $\mathcal{M}=(\alpha_{\max}-\alpha_{\min})/\Delta\alpha$, $\mathcal{N}=\tau_{\max}/\Delta\tau$, with $\Delta\alpha$ and $\Delta\tau$ denote the scale sampling interval and delay sampling interval, respectively. $\mathfrak{h}_{m,n}^{U}$ is the sampling value of the (m,n)-th grid of the discretized DSSF.

Secondly, in [7], the continuous DSSF is geometrically sampled in the scale domain and uniformly sampled in time delay domain. For $(\alpha,\tau)\in[\alpha_{\min},\alpha_{\max}]\times[0,\tau_{\max}]$, the virtual representation of the DSSF can be expressed as

$$\widetilde{h}_G\left(\alpha,\tau\right)=\sum_{m=\mathfrak{m}}^{\mathfrak{M}}\sum_{n=0}^{\mathfrak{N}(m)}\mathfrak{h}_{m,n}^{G}\delta\left(\alpha-\alpha_m'\right)\delta\left(\tau-\tau_n\right) \tag{33}$$

where $\alpha_m'=\alpha_0^m$ with a basic scale factor $\alpha_0>1$, $\mathfrak{m}=\lfloor\ln\alpha_{\min}/\ln\alpha_0\rfloor$, $\mathfrak{M}=\lceil\ln\alpha_{\max}/\ln\alpha_0\rceil$, $\mathfrak{N}(m)=\lceil\alpha_0^m B\tau_{\max}\rceil$ with B denoting the channel bandwidth, and $\mathfrak{h}_{m,n}^{G}$ is a two dimension smoothed version of the DSSF, see [7] for detail. The advantage, of sampling the scale exponentially, is that the partition mode is suitable for signal processing with wavelet transform [7], [21], [28].

This article has been accepted for publication in a future issue of this journal, but has not been fully edited. Content may change prior to final publication. Citation information: DOI 10.1109/TSP.2016.2582466, IEEE Transactions on Signal Processing

Substitute (32) or (33) into (31), we have

$$\begin{aligned} r(t) &= \int_{-\infty}^{\infty}\int_{-\infty}^{\infty}\sum_m\sum_n \mathfrak{h}_{m,n}\delta\left(\alpha-\alpha_m\right)\delta\left(\tau-\tau_n\right) \\ &\qquad\qquad \alpha_m^{\frac{1}{2}} s\left(\alpha\left(t-\tau\right)\right)d\tau d\alpha \\ &= \sum_m\sum_n \mathfrak{h}_{m,n}\alpha_m^{\frac{1}{2}} s\left(\alpha_m\left(t-\tau_n\right)\right) \end{aligned} \tag{34}$$

where $\mathfrak{h}_{m,n}=\mathfrak{h}^U_{m,n}$ for SUS pattern (32), or $\mathfrak{h}_{m,n}=\mathfrak{h}^G_{m,n}$ for SGS pattern (33).

Note that from both (2) and (34), the outputs of the MSML UWA channels can be expressed as superpositions of multiple scaled and delayed duplicates of the transmitted signal, weighted by complex amplitudes.

APPENDIX B
PROOF OF THE STATEMENT IN SECTION IV-A

The aim is to prove that the FrFT of the received signal is maximal at $u_i^\star$ when the duration of the strongest component is contained in the FrFT section. We arbitrarily pick 6 points on the time line, namely, T_0 to T_5. The chronological order is $T_0<T_1\le T_{is}<T_2<T_3<T_{ie}\le T_4<T_5$. Considering the relationship to the duration of the i-th received component, the FrFT section can be divided into the following four cases,

1) fully containing: $[T_s,T_e]=[T_1,T_4]$;
2) no containing: $[T_s,T_e]=[T_0,T_1]$ or $[T_s,T_e]=[T_4,T_5]$;
3) partially containing: $[T_s,T_e]=[T_2,T_3]$;
4) partially containing: $[T_s,T_e]$=$[T_1,T_2]$, $[T_s,T_e]$=$[T_3,T_4]$.

For the case 1), according to (17) the FrFT of the received signal with rotation angle $\phi_i^\star$, ORA of the i-th path received component, is given as

$$\begin{aligned} R_{\phi_i^\star}(u) &= \underbrace{A_i\int_{T_1}^{T_4} s_i(t)K_{\phi_i^\star}(t,u)dt}_{J_1} \\ &\quad+\sum_{l=1,l\neq i}^{L} A_l\int_{T_1}^{T_4} s_l(t)K_{\phi_i^\star}(t,u)dt \\ &\quad+\int_{T_1}^{T_4} w(t)K_{\phi_i^\star}(t,u)dt, \\ &\qquad u\in[|\csc\phi_i^\star|f_L,|\csc\phi_i^\star|f_H] \end{aligned} \tag{35}$$

where f_L and f_H, respectively, denote the lowest and highest instantaneous frequencies of the L components within $[T_1,T_4]$. With $k_i=-\cot\phi_i^\star$, J_1 in (35) can be written as

$$J_1 = A_iA_{\phi_i^\star}e^{j(\varphi_{0i}+\pi u^2\cot\phi_i^\star)}\underbrace{\int_{T_{is}}^{T_{ie}} e^{j2\pi(f_{0i}-u\csc\phi_i^\star)t}dt}_{J_2}, \tag{36}$$

where $f_{0i}=\alpha_if_0-k_i\tau_i$, $\varphi_{0i}=\pi k_i\tau_i^2-2\pi f_{0i}\alpha_i\tau_i+\varphi_0$, and the integration limit of J_1 is changed to $[T_{is},T_{ie}]$ since $s_i(t)$ is zero outside this range. The term J_2 is actually the Fourier transform of a rectangular window. Note that $\alpha_iT=T_{ie}-T_{is}$, J_2 can be written as

$$\begin{aligned} J_2 &= \alpha_iTe^{-j\pi(T_{is}+T_{ie})(f_{0i}-u\csc\phi_i^\star)} \\ &\qquad\cdot\mathrm{sinc}\big(\pi\alpha_iT(f_{0i}-u\csc\phi_i^\star)\big). \end{aligned} \tag{37}$$

Let $u_i^\star=f_{0i}\sin\phi_i^\star$, J_1 in (36) can be written as

$$J_1 = A_iC_i(u)\mathrm{sinc}\big(b_i\left(u-u_i^\star\right)\big) \tag{38}$$

where

$$\begin{aligned} C_i(u) &= A_{\phi_i^\star}\alpha_iT \\ &\qquad\cdot e^{j(\varphi_{0i}+\pi u^2\cot\phi_i^\star)-j\pi(T_{is}+T_{ie})(f_{0i}-u\csc\phi_i^\star)} \end{aligned} \tag{39}$$

is a complex coefficient, and

$$b_i=\pi\alpha_iT\csc\phi_i^\star \tag{40}$$

is a scaling factor of the sinc function in (38). The sinc function gets shaper, tending to be a narrow pulse, as the value of b_i increases. In fact, combining (40) and (9), we can see that large modulation slope leads to large $\csc\phi_i^\star$, thus leads to large b_i. Also, since α_i is closed to 1, we have $\alpha_iT\approx T$. Therefore large T leads to large b_i as well.

Obviously, even if the other components share the same ORA, i.e., $\phi_l^\star=\phi_i^\star$ for $l\neq i$, the absolute value of $R_{\phi_i^\star}(u)$ in (35) will maximize at $u=u_i^\star$ since $|A_i|>|A_l|$, $l\neq i$.

For the case 2), it is straightforward to conclude that $J_1=0$ since $s_i(t)=0$ for the integral interval of (35).

For the case 3), from the Parseval relation [20], we have

$$\int_{T_2}^{T_3}|A_is_i(t)|^2dt<\int_{T_1}^{T_4}|A_is_i(t)|^2dt=\int_{|\csc\phi_i^\star|f_L}^{|\csc\phi_i^\star|f_H}|J_1|^2du. \tag{41}$$

Since the signal energy is concentrated at the impulse in the FrFT domain, it is easily to infer that the maximum of $|R_{\phi_i^\star}(u)|$ in case 3) is smaller than that in case 1).

Finally, by combining case 2) and case 3), the proof for case 4) is trivial.

REFERENCES

[1] M. Stojanovic and J. Preisig, "Underwater acoustic communication channels: Propagation models and statistical characterization," *IEEE Communications Magazine*, vol. 47, no. 1, pp. 84–89, January 2009.

[2] P. van Walree and R. Otnes, "Ultrawideband underwater acoustic communication channels," *IEEE Journal of Oceanic Engineering*, vol. 38, no. 4, pp. 678–688, Oct 2013.

[3] P. Qarabaqi and M. Stojanovic, "Statistical characterization and computationally efficient modeling of a class of underwater acoustic communication channels," *IEEE Journal of Oceanic Engineering*, vol. 38, no. 4, pp. 701–717, 2013.

[4] F. Hlawatsch and G. Matz, *Wireless Communications over Rapidly Time-Varying Channels*. Elsevier Ltd., 2011.

[5] S. Mason, C. Berger, S. Zhou, and P. Willett, "Detection, synchronization, and doppler scale estimation with multicarrier waveforms in underwater acoustic communication," *IEEE Journal on Selected Areas in Communications*, vol. 26, no. 9, pp. 1638–1649, December 2008.

[6] C. R. Berger, S. Zhou, J. C. Preisig, and P. Willett, "Sparse channel estimation for multicarrier underwater acoustic communication: From subspace methods to compressed sensing," *IEEE Transactions on Signal Processing*, vol. 58, no. 3, pp. 1708–1721, 2010.

[7] Y. Jiang and A. Papandreou-Suppappola, "Discrete time-scale characterization of wideband time-varying systems," *IEEE Transactions on Signal Processing*, vol. 54, no. 4, pp. 1364–1375, 2006.

[8] A. R. Margetts, P. Schniter, and A. Swami, "Joint scale-lag diversity in wideband mobile direct sequence spread spectrum systems," *IEEE Transactions on Wireless Communications*, vol. 6, no. 12, pp. 4308–4319, 2007.

[9] N. F. Josso, J. J. Zhang, and et al., "On the characterization of time-scale underwater acoustic signals using matching pursuit decomposition," in *OCEANS 2009, MTS/IEEE Biloxi-Marine Technology for Our Future: Global and Local Challenges*. IEEE, 2009, pp. 1–6.

[10] S. Yerramalli and U. Mitra, "Optimal resampling of ofdm signals for multiscale–multilag underwater acoustic channels," *IEEE Journal of Oceanic Engineering*, vol. 36, no. 1, pp. 126–138, 2011.

[11] D. Cowell and S. Freear, "Separation of overlapping linear frequency modulated (lfm) signals using the fractional fourier transform," *IEEE Transactions on Ultrasonics, Ferroelectrics, and Frequency Control*, vol. 57, no. 10, pp. 2324–2333, October 2010.

[12] B. Cheng, H. Zhang, J. Xu, and G. Tang, "Bat echolocation signal processing based on fractional fourier transform," in *2008 International Conference on Radar*, Sept 2008, pp. 460–463.

[13] Y. Ma and Y. Kong, "Frft based on joint estimation time delay and radial velocity of underwater target," in *3rd International Congress on Image and Signal Processing (CISP)*, vol. 9, Oct 2010, pp. 4074–4078.

[14] H. xin Zhang, H. da Liu, S. Chen, Y. Zhang, and X. ying Wang, "Parameter estimation of chirp signals based on fractional fourier transform," *The Journal of China Universities of Posts and Telecommunications*, vol. 20, Supplement 2, pp. 95–100, 2013.

[15] P. Leong, T. Abhayapala, and T. Lamahewa, "Multiple target localization using wideband echo chirp signals," *IEEE Transactions on Signal Processing*, vol. 61, no. 16, pp. 4077–4089, Aug 2013.

[16] L. Zheng and D. Shi, "Maximum amplitude method for estimating compact fractional fourier domain," *IEEE Signal Processing Letters*, vol. 17, no. 3, pp. 293–296, March 2010.

[17] R. Chen and Y. Wang, "A novel parameter estimation method of chirp signal based on fractional fourier transform," in *2011 6th International ICST Conference on Communications and Networking in China (CHINACOM)*, Aug 2011, pp. 82–87.

[18] R. Tao, Y.-L. Li, and Y. Wang, "Short-time fractional fourier transform and its applications," *IEEE Transactions on Signal Processing*, vol. 58, no. 5, pp. 2568–2580, May 2010.

[19] V. Namias, "The fractional order fourier transform and its application to quantum mechanics," *IMA Journal of Applied Mathematics*, vol. 25, no. 3, pp. 241–265, 1980.

[20] L. Almeida, "The fractional fourier transform and time-frequency representations," *IEEE Transactions on Signal Processing*, vol. 42, no. 11, pp. 3084–3091, Nov 1994.

[21] T. Xu, Z. Tang, G. Leus, and U. Mitra, "Multi-rate block transmission over wideband multi-scale multi-lag channels," *IEEE Transactions on Signal Processing*, vol. 61, no. 4, pp. 964–979, 2013.

[22] C. Capus and K. Brown, "Short-time fractional fourier methods for the time-frequency representation of chirp signals," *The Journal of the Acoustical Society of America*, vol. 113, no. 6, pp. 3253–3263, 2003.

[23] H. Ozaktas, O. Arikan, M. Kutay, and G. Bozdagt, "Digital computation of the fractional fourier transform," *IEEE Transactions on Signal Processing*, vol. 44, no. 9, pp. 2141–2150, Sep 1996.

[24] A. Hein, *Processing of SAR Data: Fundamentals, Signal Processing, Interferometry*, 1st ed. Springer Publishing Company, 2010.

[25] Y. Zhao, H. Yu, G. Wei, F. Ji, F. Chen, and J. Zhang, "FRFT-based parameter estimation of time-varying wideband underwater acoustic multipath channels," in *10th International Conference on Underwater Networks & Systems (WUWNET '15)*, Oct. 2015, pp. 9:1–9:8.

[26] L. Weiss, "Wavelets and wideband correlation processing," *IEEE Signal Processing Magazine*, vol. 11, no. 1, pp. 13–32, Jan 1994.

[27] W. Bajwa, J. Haupt, A. Sayeed, and R. Nowak, "Compressed channel sensing: A new approach to estimating sparse multipath channels," *Proceedings of the IEEE*, vol. 98, no. 6, pp. 1058–1076, June 2010.

[28] L. Yu and L. B. White, "Optimum receiver design for broadband doppler compensation in multipath/doppler channels with rational orthogonal wavelet signaling," *IEEE Transactions on Signal Processing*, vol. 55, no. 8, pp. 4091–4103, 2007.

Yanbo Zhao received the B.S. degree in electronic science and technology from Guangxi University, China, in 2009. He is currently pursuing the Ph.D. degree in communication and information system at South China University of Technology, GuangZhou, China. His research interests include wireless digital communications, underwater acoustic communications, ultra-wide band communications and compressed sensing.

Hua Yu (M'06) received the B.S. degree in mathematics from the Southwest University, Chongqing, China, in 1995, and the Ph.D. degree in communication and information system from South China University of Technology, GuangZhou, China, in 2004.

He was a visiting scholar at the School of Marine Science and Policy, University of Delaware, USA, from August 2012 to August 2013. Currently, he is a Professor at the School of Electronic and Information Engineering, South China University of Technology. He is also the Director of Department of Underwater Communications, National Engineering Technology Research Center for Mobile Ultrasonic Detection. He was the Publication Chair and the Technical Program Committee (TPC) member of the 11th IEEE International Conference on Communication Systems in 2008. His research interests are in the physical layer technologies of wireless communications and underwater acoustic communications.

Gang Wei (M'92–SM'09) received the B.S. degree from Tsinghua University, Beijing, China, and the M.S. and Ph.D. degrees from the South China University of Technology, Guangzhou, China, in 1984, 1987, and 1990, respectively.

He was a Visiting Scholar with the University of Southern California, Los Angeles, from June 1997 to June 1998. He is currently a Professor with the School of Electronic and Information Engineering, South China University of Technology. He is a Committee Member of the National Natural Science Foundation of China. His research interests include digital signal processing and communications.

Fei Ji (M'06) received the B.S. degree in applied electronic technologies from Northwestern Polytechnical University, Xi'an, China, and the M.S. in bioelectronics and Ph.D. degrees in circuits and systems both from the South China University of Technology, Guangzhou, China, in 1992, 1995, and 1998, respectively.

She was a Visiting Scholar with the University of Waterloo, Canada, from June 2009 to June 2010. She worked in the City University of Hong Kong as a Research Assistant from March 2001 to July 2002 and a Senior Research Associate from January 2005 to March 2005. She is currently a Professor with the School of Electronic and Information Engineering, South China University of Technology. She was the Registration Chair and the Technical Program Committee (TPC) member of IEEE 2008 International Conference on Communication System. Her research focuses on wireless communication systems and networking.

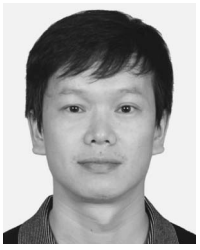

Fangjiong Chen (M06) received the BS degree in electronics and information technology from Zhejiang University, Hangzhou China, in 1997 and the Ph.D. degree in Communication and Information Engineering from South China University of Technology, Guangzhou China, in 2002.

After graduation, he joined the school of electronics and information engineering, South China University of Technology. He was a lecturer in 2002-2005 and associate professor in 2005-2011. He is currently a full-time professor in School of Electronics and Information Engineering, South China University of Technology. He is also the director of Department of Underwater Detection and Imaging, National Engineering Technology Research Center for Mobile Ultrasonic Detection. His research focuses on signal detection and estimation; array Signal Processing and wireless communication.

Prof. Chen received the National Science Fund for Outstanding Young Scientists in 2013, and was elected in the New Century Excellent Talent Program of Ministry of Education of China in 2012.